Enhancement of pea protein solubility and thermal stability for acidic beverage applications via endogenous Maillard-induced glycation and chromatography purification

Alissa A. Schneider, Fan Bu, Baraem P. Ismail[*]

Food Science and Nutrition Department, University of Minnesota, 1334 Eckles Ave, Saint Paul, Minnesota, 55108, USA

ABSTRACT

A clean-label process to endogenously glycate and purify pea protein was investigated. The production of maltodextrin from pea starch with a specific dextrose equivalent (DE) was optimized. The produced maltodextrin (14.6 DE) was used to initiate a limited and controlled Maillard-induced glycation of pea protein. The partially glycated pea protein (PG-PP) was subjected to hydrophobic interaction chromatography to remove unreacted carbohydrate, followed by characterization of the purified product. The extent of Maillard-induced glycation was monitored by assessing changes in color, free amino groups, and protein/glycoprotein profiles. The purified PG-PP was evaluated for thermal denaturation, surface properties, protein secondary structure, protein solubility, thermal stability, and digestibility. Maillard-induced glycation was limited to initial stages and resulted in a moderate blockage of amine groups (~30%). The purified PG-PP had a relatively low surface hydrophobicity, a markedly enhanced protein solubility (~90%) at pH 3.4, and a nonimpacted protein *in vitro* digestibility (~100%). This work provided the impetus needed for future scale-up and process optimization for the production of value-added pea protein ingredient intended for high protein beverage applications.

1. Introduction

Demand for high protein food and beverage products has considerably increased in recent years, mainly due to health benefits. Food and beverage manufacturers have responded to this demand by accelerating the development of new high protein products to boost their sales (Kamp, 2020). Sales of plant protein products, specifically, are expanding as consumers increasingly identify as vegans, vegetarians, or flexitarians. Historically, soy protein has dominated the plant protein market. However, manufacturers are seeking other plant protein sources, due to an unprecedented yet negative consumer perception of soy as a genetically modified (GM) crop and major allergen. Accordingly, pea protein has emerged as the most prominent alternative to soy protein (Brewster, 2020), with a global market projected to reach $555 million in 2028 (Grand View Research, 2021). While pea protein has acceptable nutritional quality, it generally has inferior functionality compared to soy protein, limiting their utilization in various food and beverage applications.

Among the plant protein food and beverage products, ready-to-drink (RTD) beverages is a major sector in the global market, which is

expected to reach a value of USD 2.3 billion by 2028, at a CAGR of 7.72% (SkyQuest, 2022). Compared to whey and soy protein, pea protein exhibits inferior solubility and thermal stability, making incorporation of pea protein into high-protein RTD beverages particularly challenging. A protein must withstand the processing steps during beverage production, including dispersion/hydration, homogenization, and thermal processing (Paulsen, 2009). Moreover, the beverage must remain stable (i.e., protein remains in solution) over its shelf life. A "high" protein claim can only be made for RTD protein beverages containing ≥4.2% biologically available protein (w/v) (21 C.F.R. § 101.54, 2022). Such high protein inclusion levels contribute to limited protein-water interactions and enhanced protein-protein interactions, thereby reducing the product's shelf life (Bogahawaththa et al., 2019). RTD protein beverages are often formulated at acidic pH (pH < 3.5) to reduce the severity of the thermal treatments, while maintaining product safety, flavor, color, stability, and nutritional value (Liu et al., 2021; Paulsen, 2009). Pea protein has very low solubility at an acidic pH, near its isoelectric point (pH 4–5) (Hansen, 2020; Liang and Tang, 2013), especially post thermal treatment (e.g., pasteurization), resulting in aggregation and sedimentation over storage (Lu et al., 2020;

* Corresponding author.
  E-mail address: bismailm@umn.edu (B.P. Ismail).

Vogelsang-O'Dwyer et al., 2021).

A variety of physical, chemical, and enzymatic processes have been investigated to modify pea protein structure to improve its solubility and thermal stability (Barac et al., 2012; Bogahawaththa et al., 2019; He et al., 2021). Of these processes, only enzymatic hydrolysis has been commercialized. However, enzymatic hydrolysis is limited by its adverse effect on sensory perception, mainly bitterness and astringency (Arteaga et al., 2020; Barac et al., 2012; Beecher et al., 2008). Therefore, other modification methods that are industrially feasible need to be explored.

Maillard-induced glycation is an alternative protein modification technique that employs the Maillard reaction (Wang and Ismail, 2012), which is a prevalent, natural reaction in many food products (Martins et al., 2000). This technique involves the controlled formation of a stable glycated protein in the early stage of the Maillard reaction (Kutzli et al., 2021). Protein glycation is achieved by incubating the protein with excess reducing carbohydrate under controlled environmental conditions (de Oliveira et al., 2016; Wang and Ismail, 2012). Glycating a protein with oligosaccharides/polysaccharides, rather than small saccharides, limits the reaction rate and its propagation to advanced undesirable stages (Wang and Ismail, 2012; Zha et al., 2020). Pea protein glycated with gum Arabic and with maltodextrin showed improved functionality (Kutzli et al., 2020; Zha et al., 2021). Pea protein glycated with arabinose and inulin had modest improvement in solubility (Chen et al., 2022; Jiang et al., 2022). Jiang et al. (2022) observed an enhancement in solubility over a wide range of pH (2–11); however, protein solubility of the glycated protein at acidic pH was still relatively low (15% solubility) at only 0.1% protein, which is much lower than the target for RTD beverages. Accordingly, there is still plenty of room for improvement in protein solubility and thermal stability at an acidic pH.

Current limitations of Maillard-induced glycation have prevented its commercialization, despite the reported research that showed consistent, yet modest, improvement in protein solubility and thermal stability. Optimization of glycation conditions and protein purification is needed to improve the industrial feasibility of this approach. Additionally, poor consumer perception of the exogenous hydrocolloids (e.g., gums, carrageenan, corn dextran, corn maltodextrin), commonly employed in this reaction, potentially limit the utilization of such a modified protein ingredient. Thus, efforts to improve the "clean label" appeal of glycated proteins are needed. One promising solution would be leveraging the endogenous starch in pea flour. Pea starch can be converted to a reducing oligosaccharide (<20 monosaccharide units) that could be used to glycate the pea protein.

Further, purification of a partially glycated protein and the removal of excess, unreacted carbohydrate is necessary yet rarely performed. Excess carbohydrate in the modified protein ingredient can adversely alter the ingredient's functionality (e.g., increase viscosity in beverages), shorten the shelf life (due to progression of chemical reactions), and reduce the protein purity. To date, the development of a clean-label process to endogenously glycate and purify pea protein has not been attempted. Therefore, the objectives of this work were: 1) develop a method to produce pea maltodextrin with a specific reducing power; 2) initiative and control the early stage of the Maillard reaction to partially glycate pea proteins with pea maltodextrin; 3) characterize the effect of glycation coupled with purification on the protein structure and the consequent impact on its solubility and thermal stability at acid pH.

2. Materials and methods

2.1. Materials

Yellow pea flour was provided by AGT Foods (Regina, SK, Canada) and commercial pea protein isolate (cPPI, ProFam® Pea 580, 79.5% protein) was provided by Archer Daniels Midland (ADM) (Decatur, IL, USA). Bacterial α-amylase (BAN® 480 LS, 528 KNU–B/g activity) was kindly provided by Novozymes North America, Inc. (Franklinton, NC,

USA). SnakeSkin™ dialysis tubing (3.5 kDa molecular weight cut-off (MWCO)), Sartorius Vivaflow® 200 Crossflow Cassettes (3 kDa MWCO), Imperial™ Protein Stain, a Pierce™ BCA assay kit, and a Pierce™ glycoprotein staining kit were purchased from Thermo Fisher Scientific Inc. (Waltham, MA, USA). Criterion™ TGX™ 4–20% precast gels, Laemmli sample buffer, 10X Tris/Glycine/sodium dodecyl sulfate running buffer, and Precision Plus Protein™ molecular weight (MW) marker were purchased from Bio-Rad Laboratories, Inc. (Hercules, CA, USA). Octyl Sepharose™ 4 Fast Flow hydrophobic interaction chromatography (HIC) resin was purchased from GE Healthcare Bio-Sciences (Uppsala, Sweden). O-phthaldialdehyde and 8-anilino-1-naphthalene-sulfonic acid (ANS) were purchased from MilliporeSigma (St. Louis, MO, USA). A Protein Digestibility Assay Kit (K-PDCAAS) was purchased from Megazyme International Co. (Bray, Ireland).

2.2. Preliminary method development

In situ enzymatic hydrolysis of starch granules in pea flour led to extensive denaturation and polymerization of the legumin proteins (Fig. S1), which would adversely impact the protein functionality. Additionally, the high molecular weight (HMW) starch and fiber in the flour resulted in challenges during protein purification following HIC. Accordingly, the endogenous starch granules in the starch rich fraction, produced during the pH extraction of pea protein, was separately hydrolyzed to produce maltodextrin with a targeted dextrose equivalent (DE).

2.3. Preparation of pea protein isolate and recovery of the starch fraction

Native pea protein isolate (nPPI) and a starch-rich fraction were produced from pea flour, following a pH-based protein extraction. Protein solubilization and precipitation were performed at pH 7.5 and 4.5, respectively, following the method reported by Bu et al. (2022) and Hansen et al. (2022), with no modification. The residual starch-rich fraction remaining after protein solubilization was collected and lyophilized. The protein content of nPPI (86.0%) and the starch-rich fraction (2.8%) was determined following the Dumas method (AOAC 990.03), using a Leco® FP828 nitrogen analyzer (LECO, St. Joseph, MI, USA), with a conversion factor of 6.25.

2.4. Production of pea maltodextrin

Partial enzymatic hydrolysis of the lyophilized starch-rich fraction was optimized to produce pea maltodextrin. Hydrolysis of the starch-rich fraction was optimized to produce a maltodextrin product with an average DE between 10 and 20 DE. Previous Maillard-induced glycation research has shown that dextran or maltodextrin in this range of DE, was suitable for the production of a glycated protein with improved solubility (Wang and Ismail, 2012; Zha et al., 2020). Parameters including hydrolysis time, removal of small saccharides, and centrifugation were tested to produce maltodextrin with the targeted DE. To evaluated different parameters, individual suspensions of the starch-rich fraction in 2 mM CaCl$_2$ double distilled water (DDW) (8.6 g in 100 mL) were prepared in triplicate, heated to 95 °C at a rate of 10 °C/min in a Brabender® Micro Visco-Amylo-Graph (MVAG) (C.W. Brabender® Instruments, Inc., Hackensack, NJ, USA), and held for 5 min to gelatinize the starch granules. Each slurry was transferred to a preheated 250 mL jacketed beaker and stirred on a magnetic stir plate until the temperature reached 75 °C, followed by the addition of α-amylase (1.1%, g enzyme/g starch-rich fraction). After incubation for 5, 10, 20, 30, 40, 50, or 60 min, the enzyme was inactivated by adjusting the pH to 3.0 and holding for 5 min at 75 °C. Samples were then cooled to room temperature on ice, neutralized, and either left as is or centrifuged at 5000×g for 10 min to remove HMW constituents (fiber and large starch molecules). Additionally, samples were then dialyzed (3.5 kDa MWCO) or ultrafiltered (3 kDa MWCO) against DDW to remove small saccharides.

All samples were lyophilized and stored at −20 °C prior to analysis. The final (optimized) procedure was repeated ~20 times to produce a bulk maltodextrin product for glycation. The DE of the produced maltodextrin was determined by the micro-Somogyi-Nelson assay using a dextrose standard curve (0.1–0.6 mM) (Shao and Lin, 2018).

2.5. Maltodextrin chain-length distribution by high-performance anion-exchange chromatography with pulsed amperometric detection (HPAEC-PAD)

The chain-length distribution of the produced maltodextrin was determined as outlined by Okyere et al. (2022), with adjustments in sample preparation. Maltodextrin (2.0 mg) was dissolved in 90% DMSO (100 μL), in septuplicate, and stirred overnight at room temperature. The final maltodextrin concentration of 2 mg/mL was obtained by adding 90% DMSO. An aliquot (25 μL) was analyzed by HPAEC-PAD using a Dionex™ ICS-5000+ HPAEC system (Dionex Corporation, Sunnyvale, CA, USA) equipped with a CarboPac™ PA100 ion-exchange column (4 × 250 mm) and accompanying guard column (4 × 50 mm). Peak areas were integrated and corrected to carbohydrate concentration (Koch et al., 1998), and the average degree of polymerization (DP) was estimated as described by Bertoft et al. (2008).

2.6. Preparation of partially glycated pea protein isolate (PG-PP)

nPPI was mixed with maltodextrin (1:4, w/w), dissolved (1:4 w/v) in potassium phosphate buffer (0.01 M, pH 7), and lyophilized. The lyophilized powder (nPPI and maltodextrin, nPPI + MD) was evenly spread in an approximately 0.0415 g/cm^2 thick layer in petri dishes. In at least triplicates, the samples were incubated in a climate chamber (HPP260, Memmert®, Büchenbach, Germany) at 49.0% relative humidity (RH) and 60 °C for 24 h to initiate a controlled and limited Maillard reaction. These conditions were selected based on the observations by Walter et al. (2016) and Wang and Ismail (2012). The 24 h-incubation period was chosen based on several glycation pre-trials, while considering loss of free amino groups. The protein content of PG-PP (17.8%) was determined by the Dumas method, and the samples were stored at −20 °C.

2.7. Assessment of glycation extent

2.7.1. Color analysis
The color of all protein samples (nPPI, nPPI + MD, PG-PP) was measured in at least triplicate, using a Chroma Meter CR-221 (Minolta Camera Co., Osaka, Japan), as outlined by Bu et al. (2022). Measurements were recorded using the CIE (International Commission on Illumination) 1976 L* a* b* color system.

2.7.2. Percent free amino groups
Percent of free amino groups in nPPI, nPPI + MD, and PG-PP was determined following the o-phthaldialdehyde (OPA) method (Goodno et al., 1981), with the exception of preparing the sample solutions (1% w/v) in 3% sodium dodecyl sulfate (SDS). The free amino group concentration (μg/mL) was determined using L-lysine standard curve and adjusted for sample protein content (μg/mL) to calculate the percent (%) free amino groups. Percent (%) loss in free amino groups of PG-PP was determined in comparison to nPPI.

2.7.3. Protein and glycoprotein profiling by gel electrophoresis
The protein and glycoprotein profile of nPPI, nPPI + MD, and PG-PP was visualized using sodium dodecyl polyacrylamide gel electrophoresis (SDS-PAGE) (Boyle et al., 2018). Protein MW marker (9 μL) and samples (5 μL, ~10 μg protein) were loaded onto a 4–20% Tris-HCl gradient gel and electrophoresed. The gel was either stained for protein with Imperial™ Protein Stain (Coomassie brilliant blue R-250) or stained for glycoprotein with the Pierce™ glycoprotein staining kit (periodic

acid-Schiff method). Gels were imaged using the Molecular Imager Gel XR system (Bio-Rad Laboratories).

2.8. Removal of unreacted maltodextrin and protein purification by HIC

Removal of unreacted maltodextrin in PG-PP by HIC was performed using a Shimadzu high-performance liquid chromatography (HPLC) system, equipped with a LC-6AD pump, a SPD-20AV UV/Vis detector, and a CMB-20A communication module (Shimadzu Corp., Kyoto, Japan). A GE HiScale™ 50/20 column (GE Healthcare Bio-Sciences, Uppsala, Sweden) was packed with Octyl Sepharose™ 4 Fast Flow HIC resin up to an approximately 7.5 cm bed height (~150 mL total column volume, CV) and equilibrated with 2 M ammonium sulfate (pH 7.0). A PG-PP (8 mL, ~3% protein, w/v in 1 M ammonium sulfate), adjusted to pH 8 (to ensure protein solubilization), was injected onto the column and run at a flow rate of 15 mL/min, with UV detection at 280 nm. The elution was performed with a 3 CV 2 M ammonium sulfate wash to remove unreacted carbohydrates, followed by a 3 CV DDW wash to collect water soluble protein, and a 3 CV 0.1 M NaOH wash/cleaning to remove hydrophobic proteins that bind strongly to the column. This procedure was repeated until enough protein was collected for all structural and functional testing. The purified, water-fraction of PG-PP (PW-PG-PP) (constituting soluble glycated and non-glycated proteins) was collected, neutralized, dialyzed against DDW, lyophilized, and stored at −20 °C. Additionally, the protein fraction that eluted with 0.1 M NaOH, referred to as the purified, NaOH fraction of PG-PP (PN-PG-PP), was collected and processed the same way as the PW-PG-PP fraction, to evaluate structural differences between the two protein fractions. Removal of unreacted carbohydrates in PG-PP was monitored by collecting 10-min interval fractions and measuring the total carbohydrate content (glucose equivalent) according to the phenol-sulfuric acid method (Nielsen, 2017).

2.9. Protein, total carbohydrate, and ash content

The protein content of reference samples (cPPI, nPPI) and purified samples (PW-PG-PP, PN-PG-PP), total carbohydrate content, expressed as percentage total carbohydrates (glucose equivalent), and ash content, were determined, in duplicates, following the Dumas method, the phenol-sulfuric acid method, and AOAC method 942.05, respectively.

2.10. Protein structural characterization

2.10.1. Thermal denaturation by differential scanning calorimetry (DSC)
The protein denaturation temperature and enthalpy of cPPI, nPPI, and PW-PG-PP were determined, in triplicate, using a Mettler Toledo DSC instrument (DSC 1 STARe System, Mettler Toledo, Columbus, OH, USA) (Bu et al., 2022). Thermograms were recorded and endothermic peaks were manually integrated to obtain the denaturation temperature and enthalpy of denaturation for each sample using a Mettler Toledo STARe Software version 11.00.

2.10.2. Protein surface properties
The surface hydrophobicity of cPPI, nPPI, PW-PG-PP, PN-PG-PP was determined, in triplicate, using a spectrofluorometric method that utilizes an 8-anilino-1-naphthalenesulfonic acid (ANS) probe (Bu et al., 2022). Net relative fluorescence index (RFI) was plotted against percent protein concentration and the slope was used as an index of protein surface hydrophobicity. As an indication of surface charge, zeta potential of protein solutions (0.1% protein, w/v in DDW), prepared at either pH 3.4 or 7.0, was measured using a dynamic light scattering instrument (Malvern Nano Z-S Zetasizer) (Bu et al., 2022).

2.10.3. Protein secondary structures by attenuated total reflectance Fourier transform infrared spectroscopy (ATR-FTIR)
ATR-FTIR spectra of cPPI, nPPI, and PW-PG-PP were recorded using

a Fourier transform infrared spectrometer (Thermo Scientific™ Nicolet™ iS50 FTIR) (Bu et al., 2022). ATR spectra were converted to transmission spectra using OMNIC® software and the second derivative of the Amide I band (1600 cm^{-1} to 1700 cm^{-1}) was obtained by PeakFit v.412 software to identify secondary structures, α-helix, β-sheet, β-turn, and random coil, and determine their distribution.

2.11. Protein solubility and thermal stability

The protein solubility of cPPI, nPPI, and PW-PG-PP was determined, in triplicate, as described by Wang and Ismail (2012). To assess the suitability for acidic, high-protein beverages, the samples were evaluated at pH 3.4 and at 5% protein (w/v in DDW). The protein solutions were stirred for 1 h at room temperature, followed by pH adjustment and another hour of stirring prior to analysis. The impact of heating at 80 °C for 30 min on the protein solubility was also evaluated. Protein solubility was expressed as the percentage of soluble protein compared to the total protein (present in the initial sample), as determined following the Dumas method.

2.12. Protein digestibility

The *in vitro* protein digestibility of cPPI, nPPI, and PW-PG-PP was determined using a Megazyme Protein Digestibility Assay Kit (K-PDCAAS) and partial amino acid composition (Table S1). Partial amino acid composition (all amino acids besides cysteine, methionine, and tryptophan) analysis was performed by the Agricultural Utilization Research Institute (AURI®, Marshall, MN, USA) following the AOAC method 996.12.

2.13. Statistical analysis

Analysis of variance (ANOVA) and t-tests were performed using IBM SPSS Statistics software version 27.0 for Windows (SPSS Inc., Chicago, IL, USA). Tukey-Kramer Honest Significant Difference (HSD) multiple means comparison test was used to determine significant differences ($P \leq 0.05$) among means. Two-sample, unpaired *t*-test was used to determine significant differences ($P \leq 0.05$) between the means of two different samples.

3. Results and discussion

3.1. Targeted production of maltodextrin

The effect of hydrolysis time, use of ultrafiltration or dialysis (small saccharide removal), and centrifugation (HMW starch/maltodextrin and fiber removal) on maltodextrin DE was evaluated. As expected, the maltodextrin DE increased with increasing hydrolysis time (Table 1). Increasing the hydrolysis time allowed for the α-amylase to further break α-(1 → 4) glycosidic linkages of starch chains, thereby creating more chains with reducing ends and increasing DE (Yusraini et al., 2013). The targeted DE range was 10–20, which would be sufficient to initiate the Maillard reaction and maintain a relatively slow rate compared to short chain saccharides. Glycation of PPI with maltodextrins was better controlled than glycation with small saccharides (glucose and lactose), which have greater reducing power (Zha et al., 2020). Small saccharides increased the rate of the Maillard reaction and its progression to undesirable, advanced stages (Zha et al., 2021). Additionally, glycation with maltodextrins of DE 10 and 18 resulted in greater improvement in protein solubility and thermal stability compared to glycation with small saccharides. Therefore, 10-min reaction time, which resulted in an average DE of ~24, was selected for further investigations.

Since the DE value of 24 was higher than the target, reducing the content of small saccharides was attempted using dialysis and ultrafiltration (UF). Both dialysis and UF, effectively reduced the content of

Table 1

Dextrose equivalent of maltodextrin production as affected by starch hydrolysis time, ultrafiltration and dialysis, and centrifugation.

Starch Hydrolysis[1]		Removal of Small Carbohydrates		Reducing power
Time	Centrifugation	Ultrafiltration	Dialysis	DE[2]
10	No	No	No	24.1[a3C4]
20	No	No	No	28.7[b]
30	No	No	No	33.0[c]
40	No	No	No	40.5[d]
50	No	No	No	49.8[e]
60	No	No	No	64.0[f]
10	No	Yes	No	13.5[aA]
10	No	No	Yes	14.6[aAB]
5	Yes	No	Yes	14.6[*]
10	Yes	No	Yes	16.2[B]

[1] Hydrolysis completed on gelatinized pea starch paste at 75 °C with 1.1% enzyme (g enzyme/g starch-rich by-product (dry basis)) in all trials.
[2] Dextrose equivalent.
[3] Lowercase letters indicate significant differences among means (n ≥ 3) within each of Trial 1 and 2 according to the Tukey-Kramer multiple means comparison test ($P < 0.05$).
[4] Uppercase letters indicate significant differences among means (n ≥ 3) within 10-min hydrolysis times according to the Tukey-Kramer multiple means comparison test ($P < 0.05$); * Designates a significant difference between means in Trial 3 as tested by a two-sample unpaired *t*-test ($P < 0.05$).

small saccharides as noted by the significantly reduced DE, with no significant differences between the two (Table 1). Lastly, an adjustment to the hydrolysis reaction time, in conjunction with the addition of a centrifugation step, was evaluated. Centrifugation was investigated to remove HMW components (starch and fiber) that remained post hydrolysis. Preliminary trials revealed challenges with sample injection through the HIC system, due to the presence of insoluble, HMW components, which clogged the column. With centrifugation and removal of these HWM components, the maltodextrin DE was expected to increase as DE is determined on a mass basis, i.e., the relative amount of reducing saccharides in a given mass would increase. Thus, a 5-min hydrolysis time, along with the previously tested 10-min time, was investigated to counter the potential increase in the average DE value post removal of HMW components. The 5-min hydrolysis time coupled with centrifugation produced maltodextrin with a significantly lower DE than the 10-min counterpart (Table 1). As theorized, the addition of the centrifugation step significantly increased the maltodextrin DE. The 5-min hydrolysis coupled with dialysis and centrifugation, therefore, were chosen as the optimal conditions to produce maltodextrin with a DE value (14.6) within that targeted range (10–20 DE).

A bulk maltodextrin sample (DE 15.7) was then produced following the optimized protocol and the chain-length distribution of the sample was evaluated. The maltodextrin chain-length distribution (Fig. 1) showed that nearly 75% of the chains fell between 2 and 20 DP, with an average of approximately 8.3 (~1.3–1.5 kDa). The term "maltodextrin" refers to a starch hydrolysis product composed of maltooligosaccharides of primarily 2–20 DP, with an average DP > 5, and between 3 and 20 DE (Dziedzic and Kearsley, 2012). Therefore, the developed process was successful in producing a maltodextrin product with the targeted characteristics for Maillard-induced glycation.

3.2. Impact of maillard-induced glycation on key characteristics

3.2.1. Effect of Maillard-induced glycation on color

Mixing of nPPI with maltodextrin prior (nPPI + MD) and post incubation (PG-PP) resulted in a significant reduction in lightness (L*), yet the difference was marginal (Table 2). Both nPPI + MD and PG-PP were significantly less green (a*) and yellow (b*) than nPPI (Table 2), attributed to the maltodextrin. A statistically significant yet visually modest decrease in lightness (L*) was observed following incubation,
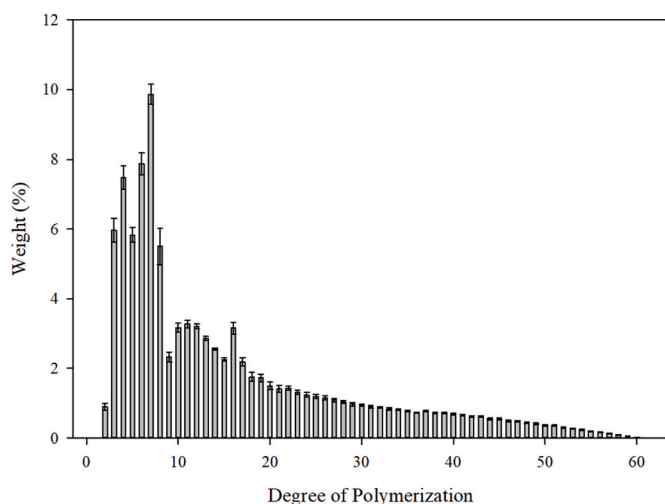
Fig. 1. Chain-length distribution of maltodextrin as determined by HPAEC-PAD. Error bars represent standard error (n = 7).

with no significant differences in a* or b* values between nPPI + MD and PG-PP (Table 2). Larger decreases in lightness (e.g., increased browning) were observed when protein-carbohydrate mixtures were incubated for longer times under more severe environmental conditions (e.g., 79% relative humidity and 80 °C) that favored higher Maillard reaction rates (Martinez-Alvarenga et al., 2014; Zha et al., 2019, 2020). Browning of various glycated pea protein products has been observed in studies utilizing dry-heating conditions (79% RH, 60 °C, ≤5 days; 75% RH, 70 °C, ≤24 h) or wet-heating conditions (80 °C, ≤24 h), especially upon extended incubation time (Kutzli et al., 2020; Zha et al., 2019, 2020). While some studies on pea protein glycation have reported browning, others did not measure change in color.

The mild dry-heating conditions (49% RH, 60 °C, 24 h) used in this experiment to induce glycation with the produced pea maltodextrin, limited the progression of the Maillard reaction to advanced stages as noted by the absence of observed browning. The success and extent of glycation are discussed in the following sections.

3.2.2. Change in free amino groups as a measure of glycation

Free amino groups content was monitored before and after incubation to assess the extent of Maillard-induced glycation. There was no statistical difference in free amino content of nPPI and the nPPI + MD control (Table 2). Upon incubation for 24 h, the free amino groups content significantly decreased, equating to a 29.6% loss in free amino groups in PG-PP compared to nPPI (Table 2). This loss was attributed to

maltodextrin chains covalently linking to available ε-amino groups of lysine residues in the early stage of the Maillard reaction (Zha et al., 2021). Comparable results were reported by Zha et al. (2019) when conjugating pea protein concentrate with gum Arabic, which resulted in approximately 20% loss in free amino groups after 24 h of incubation at 79% RH and 60 °C, and 25.9% after 72 h.

The extent of free amino group loss observed is relatively moderate, as other studies have reported much greater loss (up to ~60%) due to employing more intense Maillard reaction conditions (e.g., 65–80 °C, 70–79% RH) and carbohydrates with higher DE (Kutzli et al., 2020; Zha et al., 2019, 2020). Moreover, high loss of free amino groups could occur because of protein polymerization upon incubation at high temperatures, leading to reduced protein digestibility (Nooshkam et al., 2020; Tuohy et al., 2006). The moderate loss in free amino groups observed in this study confirmed that Maillard-inducted glycation was limited and controlled.

### 3.2.3. Effect of Maillard-induced glycation on protein and glycoprotein profiles

The protein profiles of nPPI and nPPI + MD were similar under both non-reducing and reducing conditions (Fig. 2a and b; Lanes 2–3 and 6–7). Glycoprotein staining (non-reducing conditions) revealed the presence of HMW glycoproteins (>250 kDa) in both nPPI + MD and PG-PP samples but not in nPPI (Fig. 2c; Lanes 10–12). These HMW glycoproteins, which only appeared upon mixing maltodextrin with nPPI, are likely attributed to protein conjugates that could have formed during the production of maltodextrin due to residual protein present in the starch-rich fraction. The thermal treatments (i.e., gelatinization, hydrolysis, enzyme inactivation) involved in the production of maltodextrin may have induced conjugation of residual proteins.

The protein profile of PG-PP revealed shifting upward in the molecular weight of all major globulin subunits (legumin, convicilin, and vicilin), along with longitudinal smearing under both non-reducing and reducing conditions (Fig. 2a and b; Lanes 4 and 8), confirming a successful glycation of native proteins with maltodextrin. The broadness of glycoprotein molecular weight banding depends upon the size and number of chains linked to each protein subunit, as maltodextrin is composed of maltooligosaccharides with varying chain lengths. Previous studies reported similar increases in molecular weight and heterogeneous distribution of glycated proteins (Kutzli et al., 2020; Walter et al., 2016; Wang and Ismail, 2012). Additionally, the glycated convicilin, vicilin, and legumin acidic subunit bands had greater intensity and more elevated molecular weight than the glycated 11S legumin basic subunit band (Fig. 2a and b; Lanes 4 and 8), due to higher lysine content of 7S vicilin and 8S convicilin than that of the 11S legumin (Lam et al., 2018; Zha et al., 2021).

Additionally, no heavy banding, indicative of large protein

Table 2
Color (L* a* b*), visual observation, and free amino groups (%) of native pea protein isolate (nPPI), combined nPPI and maltodextrin before incubation (nPPI + MD), and partially glycated pea protein (PG-PP).

Samples		Color			Visual Observation	Free Amino Groups
		L*	a*	b*		Free Amino Groups (%)
	nPPI	86.75[c1]	−0.36[b]	+20.00[b]		6.88[b]
Before Incubation	nPPI + MD	84.62[b]	−1.91[a]	+15.14[a]		6.77[b]
After Incubation	PG-PP	82.69[a]	−1.84[a]	+15.78[a]		4.84[a]

[1] Lowercase letters indicate significant differences among means (n ≥ 3) in each column according to the Tukey-Kramer multiple means comparison test (*P < 0.05*).
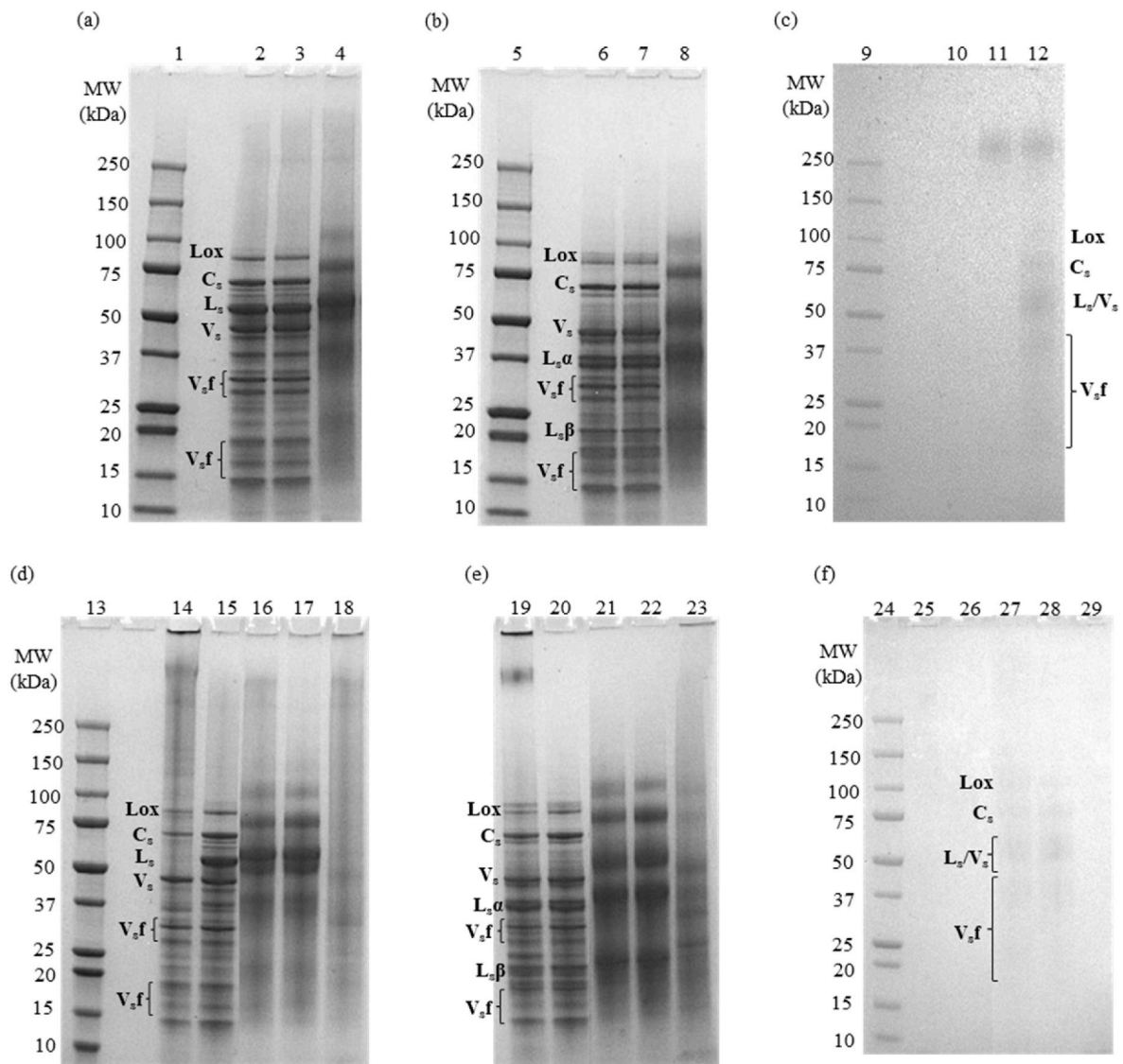
Fig. 2. SDS-PAGE visualization of the protein profiles of samples under non-reducing (a, d) and reducing (b, e) conditions using Coomassie staining, and glycoprotein profiles (c, f) of samples under non-reducing conditions using periodic acid-Schiff staining. Lanes 1, 5, 9, 13, 28: Molecular weight (MW) marker; Lanes 2, 6, 10, 15, 20, 26: nPPI; Lanes 3, 7, 11: nPPI + MD before incubation; and Lanes 4, 8, 12, 16, 21, 27: PG-PP after incubation; Lanes 14, 19, 25: cPPI; Lanes 17, 22, 28: PW-PG-PP; Lanes 18, 23, 29: PN-PG-PP. Lox: lipoxygenase; C_s: subunits of convicilin; L_s subunits of legumin; V_s: subunits of vicilin; $L_s\alpha$: acidic peptides cleaved from legumin subunits; $L_s\beta$: basic peptides cleaved from legumin subunits.

aggregates, was observed at the top of the PG-PP lane or in the loading wells under non-reducing conditions (Fig. 2a; Lane 4), contrary to previous observations where pea protein polymerization and/or the linkage of large polysaccharides (i.e., gum Arabic) have occurred under more severe glycation conditions (e.g., 65–80 °C, 70–79% RH) (Kutzli et al., 2020; Zha et al., 2019, 2020). In this study, the absence of large and insoluble aggregates suggested that the mild glycation conditions limited the Maillard reaction propagation to advanced stages. Absence of large aggregates could have a positive impact on solubility. Given the minimal change in color, moderate loss in free amino groups, and lack of protein polymerization in PG-PP, it is concluded that the Maillard reaction was successfully controlled to the initial stage, producing targeted Amadori products of pea proteins glycated with endogenous pea maltodextrin.

3.3. Evaluation of HIC-purified protein

3.3.1. Separation of unreacted maltodextrin from protein

The removal of unreacted maltodextrin from PG-PP (1:4 w/w protein to maltodextrin) was necessary to obtain a glycated protein sample with high protein purity. During HIC purification (Fig. 3a and b), Total carbohydrate content of 10-min interval fractions of eluent was monitored (Fig. 3a). Unreacted maltodextrin eluted first, followed by PW-PG-PP and PN-PG-PP (Fig. 3b). Most of the unreacted maltodextrin (~74%) was eluted with the 30-min ammonium sulfate wash (Fig. 3a, Fraction 1–3), while the remaining maltodextrin was eluted in the DDW wash (Fig. 3a, Fraction 4–6). The amount of maltodextrin in the DDW wash was mostly maltodextrin covalently linked to the proteins with residual unreacted maltodextrin. A similar distribution of recovered dextran from PG-whey protein purified following a similar HIC method was observed by Wang and Ismail (2012).

To the best of our knowledge, this is the first time that a purified PG-PP product has been produced by removing unreacted carbohydrates. It is vital to remove unreacted carbohydrates and produce a purified glycated protein ingredient for various reasons. Removal of excess carbohydrate is needed to manufacture a high purity protein ingredient that has a higher commercial value. Excess carbohydrates contribute additional calories to a product with a targeted protein claim. Excess
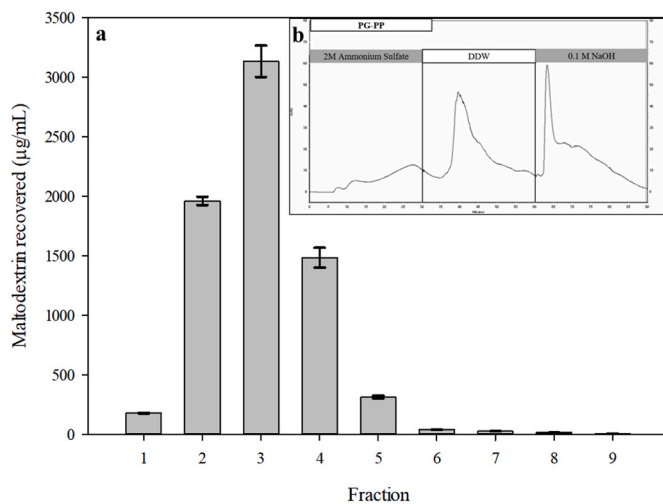
Fig. 3. Maltodextrin recovered from 10-min interval fractions, fraction 1–9, (a) collected during hydrophobic interaction chromatographic removal (b) of unreacted maltodextrin from partially glycated pea protein (PG-PP). 0–30 min: 2M ammonium sulfate wash; 30–60 min: DDW wash; 60–90 min: 0.1M NaOH wash. Error bars represent standard error (n = 2).

carbohydrates may also compete with protein for water, thereby increasing the viscosity of high protein beverages (Kennedy et al., 1995). Importantly, the Maillard reaction has the potential to progress to advanced stages over storage in the presence of unreacted reducing carbohydrates, affecting the nutritional and sensory quality of the products (Rao et al., 2012).

3.3.2. Composition of purified protein and references

The total carbohydrates and ash contents of both reference samples were relatively low (Table 3). The slight compositional difference between nPPI and cPPI could be attributed to presumed differences in extraction protocol. As intended, the HIC purified PW-PG-PP had significantly higher protein purity (~56%) than the PG-PP prior to purification (~18%). Additionally, the protein and carbohydrate content of PW-PG-PP were similar to that of PG-whey protein (~60% and 30% (w/w), respectively) purified using a similar HIC method (Wang and Ismail, 2012). PW-PG-PP had a significantly higher protein content than PN-PG-PP. While the carbohydrate and ash content were not assessed in PN-PG-PP due to limitations in sample size, it can be assumed that the remaining components of PN-PG-PP were primarily ash and carbohydrate.

3.3.3. Protein and glycoprotein profiles of purified protein and references

Differences in the protein and glycoprotein profiles of the purified protein compared to reference samples (nPPI and cPPI) were observed. Highly polymerized proteins were present in cPPI, noted by excessive

Table 3
Protein, carbohydrate, and ash contents of commercial pea protein isolate (cPPI), native pea protein isolate (nPPI), and HIC purified partially glycated pea protein (water (PW-PG-PP) and NaOH fractions (PN-PG-PP)).

Sample	Protein (%)[1]	Total carbohydrates (%)	Ash (%)
cPPI	79.5[c2]	6.81[b]	5.74[c]
nPPI	86.0[d]	2.84[a]	3.82[b]
PW-PG-PP	56.2[b]	40.91[c]	1.07[a]
PN-PG-PP	50.4[a]	N/A	N/A

[1] Percent (%) composition on a wet basis.
[2] Lowercase letters indicate significant differences among means (n = 2) in each column according to the Tukey-Kramer multiple means comparison test ($P < 0.05$).
[3] Not available.

smearing (MW > 250 kDa) and dark bands in the upper part of the gel, under both non-reducing and reducing conditions (Fig. 2d; Lane 14 and 19). The extensive aggregation is likely attributed to severe processing conditions (e.g., heat exposure, high alkalinity during protein extraction) used to produce cPPI, potentially adversely impacting its functionality (Bu et al., 2022; Shand et al., 2007). Conversely, polymerization was less apparent in nPPI, as minimal smearing was observed in the HMW region. Protein polymers were resolved under reducing conditions, indicating disulfide interactions were the primary drivers of polymerization (Fig. 2, d and e; Lane 15 and 20). With a low occurrence of protein polymerization, nPPI would potentially have better functionality than cPPI.

The PW-PG-PP protein profile closely mirrored that of PG-PP, with all major, glycated globulin subunits present in both samples in similar band intensity and proportion (Fig. 2d and e; Lanes 16–17 and 21–22). The presence of these glycated proteins in both PG-PP and PW-PG-PP was further confirmed by glycoprotein staining (Fig. 2f; Lanes 27–28). The similar protein and glycoprotein profiles suggested that most glycated proteins in PG-PP were hydrophilic, thus eluting in the water fraction. Additionally, a notable loss in HMW smearing from the PG-PP sample was observed in PW-PG-PP, rather, appearing in the PN-PG-PP sample (Fig. 2d and e; Lanes 16–18 and 21–23). The polymerized and more hydrophobic proteins in the upper lane area of PG-PP interacted with the HIC media during the ammonium sulfate and water washes, only eluting once the NaOH wash interfered with these hydrophobic interactions (O'Connor and Cummins, 2017). The NaOH wash caused ionization and increased the charge on the hydrophobic proteins, allowing them to elute. These protein polymers were assembled from unreacted major globulins through both disulfide and other covalent linkages, as smearing and a HMW band at the top of the gel remained in the PN-PG-PP sample under reducing conditions (Fig. 2e; Lane 23). However, it was noted that no glycoproteins were clearly evident in PN-PG-PP (Fig. 2f; Lane 29). This observation indicated that the majority of glycated proteins eluted in the water wash, and the concentration of glycoproteins in PN-PG-PP was probably below the threshold of the stain. The unique protein and glycoproteins profiles of PW-PG-PP and PN-PG-PP could have major implications on the protein structural characteristics and its solubility.

3.4. Structural characterization of purified protein

3.4.1. Protein denaturation

No endothermic peaks were observed in cPPI, indicating complete denaturation (Table 4), similar to the observation by Bu et al. (2022). The severe commercial processing conditions used to produce cPPI led to protein denaturation and subsequent polymerization (Fig. 2d; Lane 14). Conversely, two endothermic peaks were observed in nPPI (Table 4), corresponding to vicilin and legumin proteins, with T_d and combined enthalpy (ΔH) similar to previous observations (Bu et al., 2022). While the vicilin and legumin endothermic peaks slightly overlapped, two distinct peaks were clearly identifiable. However, the vicilin and legumin endothermic peaks in PW-PG-PP were less distinct, ultimately appearing as one endothermic peak. Shifts in thermal transitions could be attributed to structural changes in the glycated protein. Therefore, the total ΔH of both vicilin and legumin endothermic peaks in nPPI was determined in order to adequately compare the denaturation state of PW-PG-PP to that of nPPI. Although Maillard-induced glycation was expected to cause partial denaturation (Wang et al., 2013; Wang and Ismail, 2012; Zha et al., 2020), the ΔH of PW-PG-PP was not statistically different than that of nPPI (Table 4). The removal of denatured and polymerized proteins via HIC purification (Fig. 2d; Lanes 18–19) likely countered the potential, yet partial denaturation that could have been induced upon glycation, thus maintaining the ΔH of PW-PG-PP. Additionally, the midpoint temperature of the single endothermic peak was deemed as the T_d, which remained within the range of that of vicilin and legumin in nPPI (Table 4). While other

Table 4

Denaturation temperatures and enthalpy, surface hydrophobicity, surface charge, and secondary structures of commercial pea protein isolate (cPPI), native pea protein isolate (nPPI), and HIC purified partially glycated pea protein (water (PW-PG-PP) and NaOH fractions (PN-PG-PP)).

Samples	Denaturation Temperature and Enthalpy				Surface Properties			Secondary Structure			
	Denaturation Temperature			Enthalpy of Denaturation[1]	Surface Hydrophobicity	Surface Charge		ATR-FTIR			
	T_d, °C			ΔH, J g-1	RFI	pH 3.4 mV	pH 7.0 mV	α Helix	β Sheet	β Turn	Random Coil
								Relative Percentage			
	Vicilin	*Legumin*	*Vicilin/Legumin*[2]								
cPPI	~	~	~	~	13822[c]	+23.0[c]	−32.6[c]	16.6[a]	37.5[a]	32.2[a]	13.8[b]
nPPI	82.2	90.4	N/A[3]	7.92[a][4]	9245[b]	+30.1[d]	−37.1[d]	20.6[b]	43.6[b]	31.3[a]	4.5[a]
PW-PG-PP	N/A	N/A	83.4	7.82[a]	6237[a]	+20.5[b]	−21.5[b]	18.4[ab]	45.0[b]	30.7[a]	5.9[a]
PN-PG-PP	−[5]	–	–	–	9000[b]	+7.0[a]	−17.9[a]	–	–	–	–

~ No peak of denaturation observed; [1] Total enthalpy of denaturation; [2] Could not be integrated separately vicilin and legumin endothermic peaks; [3] Not applicable; [4] Lowercase letters indicate significant differences among means (n = 3) in each column according to the Tukey-Kramer multiple means comparison test ($P < 0.05$); [5] Not analyzed.

studies have found that glycation increases T_d (Chen et al., 2022; Jiang et al., 2022; Zha et al., 2020), the constant T_d observed in this study could be attributed to the distinct Maillard reaction conditions, substrates, and composition of PW-PG-PP (including a unique protein, carbohydrate, and ash/ammonium sulfate content) compared to other glycated samples. Nevertheless, this is the first study that evaluated the effect of glycation coupled with HIC purification on pea protein denaturation properties. The relatively high enthalpy and the removal of denatured and polymerized aggregates could contribute to enhanced solubility and thermal stability of PW-PG-PP.

3.4.2. Protein surface properties

Due to complete denaturation of the proteins in cPPI, its net surface hydrophobicity was significantly higher than that of nPPI (Table 4), similar to what was observed by Bu et al. (2022). This observation was attributed to the mild extraction conditions used during the production of nPPI. Glycation coupled with HIC purification resulted in significantly lower surface hydrophobicity of PW-PG-PP compared to nPPI (Table 4). Despite the unfolding that typically occurs upon Maillard-induced glycation, glycation reduces protein surface hydrophobicity through the covalent linkage of hydrophilic carbohydrates(de Oliveira et al., 2016; Wang and Ismail, 2012; Zha et al., 2021). While surface hydrophobicity has not been widely investigated in previous glycation studies, partially glycated proteins are rarely purified to remove residual carbohydrates. In this study, purification by HIC successfully fractionated the proteins in PG-PP into two fractions, with PW-PG-PP having a significantly lower surface hydrophobicity than PN-PG-PP. This observed difference in surface hydrophobicity between the two fractions likely contributed to the observed differences in the degree of protein polymerization (Fig. 2d; Lanes 17–18). The higher surface hydrophobicity enhanced attractive forces among protein molecules and facilitated further interactions via disulfide linkages. On the other hand, the surface hydrophobicity of PN-PG-PP was comparable to that of nPPI, showing that the average surface hydrophobicity of the two fractions is lower than that of nPPI. This observation confirmed the effect of glycation on reducing the overall surface hydrophobicity of pea protein, with HIC separation providing an added positive impact.

The surface charge was evaluated not only at pH 7 but also at pH 3.4 to provide a better insight to the solubility tested at pH 3.4. The surface charge of nPPI was significantly higher than that of cPPI at both pH levels, as previously reported (Bu et al., 2022; Ladjal-Ettoumi et al., 2016). Notably, regardless of pH level, PW-PG-PPI and PN-PG-PP had less net surface charge than nPPI (Table 4). Moreover, the surface charge of cPPI was significantly higher than that of the purified samples, despite the fact that cPPI was the most denatured and polymerized (Table 4, Fig. 2d; Lane 14). Residual ammonium sulfate in the HIC fractionated samples might have neutralize ionizeable groups on the surface of the protein (Zhu et al., 2022), ultimately reducing the observed surface

charge load (Lam et al., 2018). This effect was similarly observed by Bu et al. (2022) in undialyzed, modified PPI samples containing salt, and by Bogahawaththa et al. (2019) in PPI solutions with added sodium chloride. While fractionated samples in this study were dialyzed and had relatively low ash levels (PW-PG-PP <2% ash, Table 2), residual ammonium sulfate would not have been detected by the dry ashing method, as it decomposes above 280 °C. Additionally, the significantly lower net positive charge of PW-PG-PP compared to nPPI at pH 3.4 could be attributed to the covalent linkage of maltodextrin at the ε-amino groups of lysine residues that would otherwise be protonated at pH 3.4. Wang and Ismail (2012) noted that the isoelectric point of whey protein was reduced upon glycation due to the blockage of amino groups, which would explain less protonation at pH 3.4. Glycation might have also led to a reduction in the measured zeta potential (ζ) of PW-PG-PP, as the matlodextrin layer at the surface of the protein might have shielded charges on the protein, as Chen et al. (2016) observed in peanut protein isolate-maltodextrin conjugates. Although charge shielding by residual salts might have occurred in both HIC fractions, PN-PG-PP had the lowest surface charges at both pH levels and more so at pH 3.4 (Table 4). This observation is consistent with the protein profile of PN-PG-PP, which had higher surface hydrophobicity and relatively more polymerized proteins than the PW-PG-PP (Fig. 2d; Lanes 17–18).

3.4.3. Protein secondary structures

cPPI had the lowest relative abundance of α-helix and β-sheet structures and the highest abundance of random coil (Table 4), which confirmed protein denaturation at the secondary structure level due to adverse processing conditions, as noted by Bu et al. (2022). In contrast, nPPI, which was produced under mild extraction conditions, retained a significantly higher relative abundance of α-helix and β-sheet, and lower abundance of random coil, compared to cPPI. Glycation coupled with HIC purification did not result in significant differences in the distribution of the protein's secondary structures compared to nPPI. The insignificant change in protein secondary structure could partially explain the observed insignificant differences in the ΔH between PW-PG-PP and nPPI (Table 4). Others have found an increased abundance of β-sheet structure upon glycation (Li et al., 2014; Pirestani et al., 2017; Wang et al., 2013), which could have contributed to enhanced thermal stability (Damodaran and Parkin, 2017). The effect of glycation on secondary structures can potentially depend on the particular substrates, Maillard reaction conditions, and purification protocol that may alter the protein profile. The observed insignificant change in the secondary structures upon glycation and purification will, therefore, not have a direct bearing on the thermal stability of PW-PG-PP.

3.5. Impact of maillard-induced glycation and HIC-purification on protein solubility and thermal stability at pH 3.4

The protein solubility of cPPI (<14%) was significantly the lowest among the samples under non-heated and heated conditions (Table 5). This low protein solubility of cPPI is attributed to its complete protein denaturation, excessive aggregation, higher surface hydrophobicity, and lower surface charge compared to nPPI (Table 4, Fig. 2d; **Lane 14**). Similar differences in protein solubility between a commercial and lab-produced PPI have been previously reported (Bu et al., 2022; Shand et al., 2007). Upon glycation and HIC purification, the protein solubility significantly increased, with PW-PG-PP showing a remarkably high solubility (up to ~ 90%) (Table 5). The high solubility of PW-PG-PP is mostly attributed to its relatively low surface hydrophobicity, allowing for increased protein-water interaction (Damodaran and Parkin, 2017). Heating of the 5% protein solutions significantly increased the solubility of all samples, similar to the observation of Bu et al. (2022). Heating under the T_d may have imparted partial unfolding, which could have enhanced water interactions with some of the exposed functional groups. Bogahawaththa et al. (2019) reported that particular heating temperature/time combinations and environmental conditions can have unique effects on protein solubility.

While previous reports confirmed modest improvement in the solubility of pea protein glycated with gum Arabic, mono- and disaccharides, and maltodextrin (Kutzli et al., 2020; Zha et al., 2019, 2020), protein solubility was evaluated in the presence of unreacted carbohydrates (i. e., without any purification) and at very low protein concentrations (≤0.25% protein in buffer or water, w/w). Such low protein concentration is not relevant to high protein beverage applications (>4.2% of available protein). Additionally, excess, unreacted carbohydrates impede direct evaluation the impact of glycation on protein solubility. Unreacted carbohydrates may reduce protein solubility by competing with the protein for water, while imparting additional, undesired viscosity to the protein beverage (Kennedy et al., 1995; Wei et al., 2020). Additionally, while pea protein solubility was shown to be improved upon glycation, it remained less than 50% at acidic pH (around 3.4) (Jiang et al., 2022; Kutzli et al., 2020) much lower than the observed enhancement observed in this study. Therefore, this study is uniquely distinct from past reports not only in the use of endogenous pea maltodextrin, but also in the production of a partially glycated, purified pea protein that is highly soluble under conditions relevant to high-protein, RTD beverages (at 5% protein concentration), with solubility, nearly as high as that of whey protein, the gold standard for high protein beverages (Wang and Ismail, 2012). Removal of unreacted carbohydrates from PG-PP allowed for a direct analysis of protein solubility, with limited interference from excess carbohydrates.

3.6. Protein digestibility

Maillard-induced glycation with bulky carbohydrates may hinder the accessibility of digestive proteases to the binding sites, thus reducing protein digestibility and bioaccessibility of amino acids (Gumus et al., 2016; Nooshkam et al., 2020). Therefore, the impact of glycation and purification on the *in vitro* protein digestibility of PW-PG-PP was evaluated in comparison to nPPI and cPPI. All three samples demonstrated high *in vitro* protein digestibility (~100%) (Table 5). While statistically significant, the slightly lower digestibility of PW-PG-PP, compared to that of nPPI and cPPI, is not impactful, as the digestibility scores were all ≥100% (Table 5). Additionally, based on the amino acid analysis (Table S1) corrected for protein content, the lysine score, i.e. the ratio of lysine (mg/g protein) in each sample to the recommended lysine content in reference protein (mg/g protein) (based on the recommended amino acid scoring pattern for children (6 months–3 years)) was >1 (WHO, 1991). This observation indicated that glycation along with HIC purification did not reduce the amount of bioaccessible lysine. Although ~30% of lysine groups were blocked (Table 2), the lysine content as determined by the AOAC method amino acid composition was not impacted by glycation, indicating that the Maillard reaction was limited to early stages. Therefore, lysine was not degraded and the protein-carbohydrate bond would most likely remain accessible to digestive enzymes.

Digestibility of glycated proteins, has not been extensively researched. Qu et al. (2018) and Shen and Li (2021), found that rapeseed protein-dextran conjugates and pea protein-guar gum conjugates, respectively, had reduced *in vitro* digestibility upon glycation. On the other hand, glycation of whey protein and subsequent HIC purification increased protein digestibility, due to partial unfolding of the protein, which increased the accessibility of digestive enzymes (Wang and Ismail, 2012). Differences in the reported digestibility of glycated protein are likely caused by differences in the extent of glycation (i.e., number of saccharides attached to the protein molecule), the size of the linked saccharides, and changes in protein conformation.

4. Conclusion

Optimization of the hydrolysis of endogenous pea starch resulted in the production of maltodextrin with a targeted DE needed to induce limited yet controlled Maillard glycation. Pea protein glycation coupled with HIC purification was successful in producing pea protein with markedly enhanced solubility at pH 3.4 and at a protein concentration relevant for RTD high protein acidic beverages. This work can be differentiated from previous pea protein glycation studies in several ways including the utilization of endogenously produced pea maltodextrin, removal of excess unreacted carbohydrates for direct evaluation of protein solubility, and assessment of solubility at 5% protein concentration. Results confirmed moderated blockage of amine groups without complete degradation of lysine, while maintaining 100% *in vitro* digestibility. Complete elucidation of PW-PG-PP and PN-PG-PP structure and composition is needed, coupled with a mass balance determination, to better evaluate the efficiency of separation. Additionally, determining the feasibility of scaling up glycation and purification is a natural follow up study. Nevertheless, this work provided foundational information and paved the way for future investigation and optimization of endogenous glycation for the production of pea protein with added-value for application in high-protein, RTD beverages.

CRediT authorship contribution statement

Alissa A. Schneider: Conceptualization, Methodology, Execution of experiments, Investigation, Formal data analysis, Formal analysis, Data curation, Writing – original draft. **Fan Bu:** Methodology, Writing – review & editing. **Baraem P. Ismail:** Conceptualization, Project administration, Writing – review & editing, Funding acquisition.

Table 5

Solubility (%) and *in vitro* protein digestibility (%) of commercial pea protein (cPPI), native pea protein (nPPI), HIC purified partially glycated pea protein (PW-PG-PP) at pH 3.4 and 5% protein concentration.

Samples	Solubility (%)		*In vitro* Protein Digestibility (%)
	Non-heated	Heated (80 °C for 30 min)	
cPPI	8.99[a1]	13.7[a]*	108.5[b1]
nPPI	42.0[b]	61.2[b]*	109.4[b]
PW-PG-PP	75.2[c]	90.5[c]*	101.7[a]

[1] Lowercase letters indicate significant differences among means (n ≥ 2) in each column according to the Tukey-Kramer multiple means comparison test ($P < 0.05$); * Designates a significant difference between non-heated and heated samples in each row as tested by a two-sample unpaired *t*-test ($P < 0.05$).

Declaration of competing interest

The authors declare that they have no known competing financial interests or personal relationships that could have appeared to influence the work reported in this paper.

Data availability

Data will be made available on request.

Appendix A. Supplementary data

Supplementary data to this article can be found online at https://doi.org/10.1016/j.crfs.2023.100452.

References

Arteaga, V.G., Guardia, M.A., Muranyi, I., Eisner, P., Schweiggert-Weisz, U., 2020. Effect of enzymatic hydrolysis on molecular weight distribution, techno-functional properties and sensory perception of pea protein isolates. Innovat. Food Sci. Emerg. Technol. 65, 102449.

Barac, M., Cabrilo, S., Stanojevic, S., Pesic, M., Pavlicevic, M., Zlatkovic, B., Jankovic, M., 2012. Functional properties of protein hydrolysates from pea (*Pisum sativum, L*) seeds. Int. J. Food Sci. Technol. 47 (7), 1457–1467.

Beecher, J., Drake, M., Luck, P., Foegeding, E., 2008. Factors regulating astringency of whey protein beverages. J. Dairy Sci. 91 (7), 2553–2560.

Bertoft, E., Piyachomkwan, K., Chatakanonda, P., Sriroth, K., 2008. Internal unit chain composition in amylopectins. Carbohydr. Polym. 74 (3), 527–543.

Bogahawaththa, D., Chau, N.H.B., Trivedi, J., Dissanayake, M., Vasiljevic, T., 2019. Impact of selected process parameters on solubility and heat stability of pea protein isolate. LWT–Food Sci. Technol. 102, 246–253.

Boyle, C., Hansen, L., Hinnenkamp, C., Ismail, B.P., 2018. Emerging camelina protein: extraction, modification, and structural/functional characterization. J. Am. Oil Chem. Soc. 95 (8), 1049–1062.

Brewster, E., 2020. Beyond soy: formulating vegan and vegetarian foods. Food Technol. 74 (7), 55–63.

Bu, F., Nayak, G., Bruggeman, P., Annor, G., Ismail, B.P., 2022. Impact of plasma reactive species on the structure and functionality of pea protein isolate. Food Chem. 371, 131135.

Chen, L., Chen, J., Wu, K., Yu, L., 2016. Improved low pH emulsification properties of glycated peanut protein isolate by ultrasound Maillard reaction. J. Agric. Food Chem. 64 (27), 5531–5538.

Chen, X., Dai, Y., Huang, Z., Zhao, L., Du, J., Li, W., Yu, D., 2022. Effect of ultrasound on the glycosylation reaction of pea protein isolate–arabinose: structure and emulsifying properties. Ultrason. Sonochem. 89, 106157.

Damodaran, S., Parkin, K.L., 2017. Amino acids, peptides, and proteins. In: Fennema's Food Chemistry. CRC Press, pp. 235–356.

de Oliveira, F.C., Coimbra, J.S.d.R., de Oliveira, E.B., Zuñiga, A.D.G., Rojas, E.E.G., 2016. Food protein-polysaccharide conjugates obtained via the Maillard reaction: a review. Crit. Rev. Food Sci. Nutr. 56 (7), 1108–1125.

Dziedzic, S., Kearsley, M., 2012. Handbook of Starch Hydrolysis Products and Their Derivatives. Springer Science & Business Media.

Goodno, C.C., Swaisgood, H.E., Catignani, G.L., 1981. A fluorimetric assay for available lysine in proteins. Anal. Biochem. 115 (1), 203–211.

Grand View Research, 2021. Global protein ingredients market size report, 2021-2028, 1–10. Retrieved from. https://www.grandviewresearch.com/industry-analysis/protein-ingredients-market. (Accessed 11 June 2022).

Gumus, C.E., Davidov-Pardo, G., McClements, D.J., 2016. Lutein-enriched emulsion-based delivery systems: impact of Maillard conjugation on physicochemical stability and gastrointestinal fate. Food Hydrocolloids 60, 38–49.

Hansen, L., 2020. The Optimization and Scale-Up of Pea Protein Extractions and Impact on Structural and Functional Properties.

Hansen, L., Bu, F., Ismail, B., 2022. Structure-Function Guided Extraction and Scale-up of Pea Protein Isolate Production. Foods 11, 3773.

He, X., Chen, J., He, X., Feng, Z., Li, C., Liu, W., Dai, T., Liu, C., 2021. Industry-scale microfluidization as a potential technique to improve solubility and modify structure of pea protein. Innovat. Food Sci. Emerg. Technol. 67, 102582.

Jiang, W., Wang, Y., Ma, C., McClements, D.J., Liu, F., Liu, X., 2022. Pea protein isolate-inulin conjugates prepared by pH-shift treatment and ultrasonic-enhanced glycosylation: structural and functional properties. Food Chem. 384, 132511.

Kamp, K., 2020. Super Protein : Incl Impact of Covid-19- US. Retrieved from: https://store.mintel.com/report/us-super-protein-market-report. (Accessed 11 June 2022).

Kennedy, J., Knill, C., Taylor, D., 1995. Maltodextrins. In: Handbook of Starch Hydrolysis Products and Their Derivatives. Springer, pp. 65–82.

Koch, K., Andersson, R., Åman, P., 1998. Quantitative analysis of amylopectin unit chains by means of high-performance anion-exchange chromatography with pulsed amperometric detection. J. Chromatogr. A 800 (2), 199–206.

Kutzli, I., Griener, D., Gibis, M., Schmid, C., Dawid, C., Baier, S.K., Hofmann, T., Weiss, J., 2020. Influence of Maillard reaction conditions on the formation and solubility of pea protein isolate-maltodextrin conjugates in electrospun fibers. Food Hydrocolloids 101, 105535.

Kutzli, I., Weiss, J., Gibis, M., 2021. Glycation of plant proteins via maillard reaction: reaction chemistry, technofunctional properties, and potential food application. Foods 10 (2), 376.

Ladjal-Ettoumi, Y., Boudries, H., Chibane, M., Romero, A., 2016. Pea, chickpea and lentil protein isolates: physicochemical characterization and emulsifying properties. Food Biophys. 11 (1), 43–51.

Lam, A., Can Karaca, A., Tyler, R., Nickerson, M., 2018. Pea protein isolates: structure, extraction, and functionality. Food Rev. Int. 34 (2), 126–147.

Li, C., Xue, H., Chen, Z., Ding, Q., Wang, X., 2014. Comparative studies on the physicochemical properties of peanut protein isolate–polysaccharide conjugates prepared by ultrasonic treatment or classical heating. Food Res. Int. 57, 1–7.

Liang, H.-N., Tang, C.-H., 2013. pH-dependent emulsifying properties of pea [Pisum sativum (L.)] proteins. Food Hydrocolloids 33 (2), 309–319.

Liu, Y., Toro-Gipson, R.S.D., Drake, M., 2021. Sensory properties and consumer acceptance of ready-to-drink vanilla protein beverages. J. Sensory Stud. 36 (6), e12704.

Lu, Z., He, J., Zhang, Y., Bing, D., 2020. Composition, physicochemical properties of pea protein and its application in functional foods. Crit. Rev. Food Sci. Nutr. 60 (15), 2593–2605.

Martinez-Alvarenga, M., Martinez-Rodriguez, E., Garcia-Amezquita, L., Olivas, G., Zamudio-Flores, P., Acosta-Muniz, C., Sepulveda, D., 2014. Effect of Maillard reaction conditions on the degree of glycation and functional properties of whey protein isolate–Maltodextrin conjugates. Food Hydrocolloids 38, 110–118.

Martins, S.I., Jongen, W.M., Van Boekel, M.A., 2000. A review of Maillard reaction in food and implications to kinetic modelling. Trends Food Sci. Technol. 11 (9–10), 364–373.

Nielsen, S.S., 2017. Total carbohydrate by phenol-sulfuric acid method. In: Food Analysis Laboratory Manual. Springer, pp. 137–141.

Nooshkam, M., Varidi, M., Verma, D.K., 2020. Functional and biological properties of Maillard conjugates and their potential application in medical and food: a review. Food Res. Int. 131, 109003.

O'Connor, B.F., Cummins, P.M., 2017. Hydrophobic interaction chromatography. In: Protein Chromatography. Springer, pp. 355–363.

Okyere, A.Y., Boakye, P.G., Bertoft, E., Annor, G.A., 2022. Structural characterization and enzymatic hydrolysis of radio frequency cold plasma treated starches. J. Food Sci. 87 (2), 686–698.

Paulsen, P., 2009. Isolated soy protein usage in beverages. In: Functional and Speciality Beverage Technology. Elsevier, pp. 318–345.

Pirestani, S., Nasirpour, A., Keramat, J., Desobry, S., 2017. Preparation of chemically modified canola protein isolate with gum Arabic by means of Maillard reaction under wet-heating conditions. Carbohydr. Polym. 155, 201–207.

Qu, W., Zhang, X., Chen, W., Wang, Z., He, R., Ma, H., 2018. Effects of ultrasonic and graft treatments on grafting degree, structure, functionality, and digestibility of rapeseed protein isolate-dextran conjugates. Ultrason. Sonochem. 42, 250–259.

Rao, Q., Rocca-Smith, J.R., Schoenfuss, T.C., Labuza, T.P., 2012. Accelerated shelf-life testing of quality loss for a commercial hydrolysed hen egg white powder. Food Chem. 135 (2), 464–472.

Shand, P.J., Ya, H., Pietrasik, Z., Wanasundara, P.K.J.P.D., 2007. Physicochemical and textural properties of heat-induced pea protein isolate gels. Food Chem. 102 (4), 1119–1130.

Shao, Y., Lin, A.H.-M., 2018. Improvement in the quantification of reducing sugars by miniaturizing the Somogyi-Nelson assay using a microtiter plate. Food Chem. 240, 898–903.

Shen, Y., Li, Y., 2021. Acylation modification and/or guar gum conjugation enhanced functional properties of pea protein isolate. Food Hydrocolloids 117, 106686.

SkyQuest, 2022. Global RTD Protein Beverages Market. Retrieved from. https://skyquestt.com/report/rtd-protein-beverages-market. (Accessed 11 June 2022).

Tuohy, K.M., Hinton, D.J., Davies, S.J., Crabbe, M.J.C., Gibson, G.R., Ames, J.M., 2006. Metabolism of Maillard reaction products by the human gut microbiota–implications for health. Mol. Nutr. Food Res. 50 (9), 847–857.

Vogelsang-O'Dwyer, M., Zannini, E., Arendt, E.K., 2021. Production of pulse protein ingredients and their application in plant-based milk alternatives. Trends Food Sci. Technol. 110, 364–374.

Walter, J., Greenberg, Y., Sriramarao, P., Ismail, B.P., 2016. Limited hydrolysis combined with controlled Maillard-induced glycation does not reduce immunoreactivity of soy protein for all sera tested. Food Chem. 213, 742–752.

Wang, Q., He, L., Labuza, T.P., Ismail, B., 2013. Structural characterisation of partially glycosylated whey protein as influenced by pH and heat using surface-enhanced Raman spectroscopy. Food Chem. 139 (1–4), 313–319.

Wang, Q., Ismail, B., 2012. Effect of Maillard-induced glycosylation on the nutritional quality, solubility, thermal stability and molecular configuration of whey proteinv. Int. Dairy J. 25 (2), 112–122.

Wei, Y., Cai, Z., Wu, M., Guo, Y., Tao, R., Li, R., Wang, P., Ma, A., Zhang, H., 2020. Comparative studies on the stabilization of pea protein dispersions by using various polysaccharides. Food Hydrocolloids 98, 105233.

WHO, 1991. Protein Quality Evaluation: Report of the Joint FAO/WHO Expert Consultation, vol. 51. Food & Agriculture Org, Bethesda, Md., USA, pp. 4–8. December 1989.

Yusraini, E., Hariyadi, P., Kusnandar, F., 2013. Preparation and partial characterization of low dextrose equivalent (DE) maltodextrin from banana starch produced by enzymatic hydrolysis. Starch Staerke 65 (3-4), 312–321.

Zha, F., Dong, S., Rao, J., Chen, B., 2019. The structural modification of pea protein concentrate with gum Arabic by controlled Maillard reaction enhances its functional properties and flavor attributes. Food Hydrocolloids 92, 30–40.

Zha, F., Gao, K., Rao, J., Chen, B., 2021. Maillard-driven chemistry to tune the functionality of pea protein: structure characterization, site-specificity, and aromatic profile. Trends Food Sci. Technol. 114, 658–671.

Zha, F., Yang, Z., Rao, J., Chen, B., 2020. Conjugation of pea protein isolate via Maillard-driven chemistry with saccharide of diverse molecular mass: molecular interactions leading to aggregation or glycation. J. Agric. Food Chem. 68 (37), 10157–10166.

Zhu, P., Huang, W., Chen, L., 2022. Develop and characterize thermally reversible transparent gels from pea protein isolate and study the gel formation mechanisms. Food Hydrocolloids 125, 107373.